EAST EUROPEAN JOURNAL OF PHYSICS. 1. 357-362 (2026)
DOI:10.26565/2312-4334-2026-1-42 ISSN 2312-4334

IMPROVING CARBON NANOTUBE SYNTHESIS BY THE REMOVAL OF AMORPHOUS CARBON

Sevara G. Gulomjanova*, Ilyos Kh. Khudaykulov, Ilyos J. Abdisaidov, Khatam B. Ashurov
Arifov Institute of Ion-Plasma and Laser Technologies of Uzbekistan Academy of Sciences
100125, Durmon Yuli St. 33, Tashkent, Uzbekistan
**Corresponding Author e-mail: sevara@iplt.uz*
Received November 17, 2025; revised February 6, 2026; accepted February 19, 2026

In this study, carbon nanotubes (CNTs) were synthesized on Ni-coated sapphire substrates using conventional and water-assisted chemical vapor deposition (CVD and WA-CVD) methods to evaluate the effect of water vapor on amorphous carbon removal and catalyst activity at low temperatures. Reduced nickel nanocatalysts were prepared by the sol–gel method and activated in a hydrogen atmosphere. Raman spectroscopy confirmed that CNTs synthesized by WA-CVD exhibited a higher degree of graphitization (ID/IG ≈ 1.18) and the absence of amorphous carbon peaks around 794 cm^{-1}, indicating improved purity. X-ray diffraction (XRD) analysis revealed the formation of graphitic carbon (002) and Ni_3C crystalline phases, as well as a rightward shift of the (002) peak to $2\theta = 26.2°$, suggesting lattice contraction caused by water-vapor-induced stress. Transmission electron microscopy (TEM) images showed that CNTs synthesized under WA-CVD conditions were thinner (17–25 nm), longer (≥ 1 μm), and cleaner than those obtained by conventional CVD, which exhibited thick amorphous carbon coatings. These results demonstrate that the controlled addition of water vapor during CVD suppresses amorphous carbon formation, regenerates catalyst active sites, and significantly enhances CNT crystallinity and morphological uniformity. The findings provide an efficient approach for synthesizing high-purity, well-aligned CNTs suitable for thermal interface materials, nanocomposites, and electronic device applications.
Keywords: *Carbon nanotubes; Amorphous carbon removal; Water-assisted CVD; Nickel catalyst; Sol–gel synthesis; Raman spectroscopy; X-ray diffraction; TEM morphology; Graphitization degree; Catalyst regeneration*
PACS: 81.07.De; 81.15.Gh; 81.20.Fw; 61.48.De; 61.72.Cc; 78.30.Na; 61.05.cp; 68.37.Lp; 82.65.+r.

INTRODUCTION

Since their discovery by Iijima in 1991 [1], carbon nanotubes (CNTs) have been among the most promising nanomaterials investigated to date. Their exceptional mechanical strength, electrical and thermal conductivity, as well as chemical stability, make CNTs suitable for a wide range of applications, including electronics, catalysis, composite materials, energy storage systems, and thermal interface materials (TIMs) [2–4].

The quality, morphology, and properties of CNTs mainly depend on the synthesis parameters—particularly the type of catalyst, growth temperature, carbon source, and reaction atmosphere [5]. The most widely used synthesis technique is Chemical Vapor Deposition (CVD), which offers several advantages such as simple technological requirements, low cost, and controllable growth conditions [6,7]. However, the formation of amorphous carbon (a-C) during the CVD process significantly reduces the structural and functional quality of CNTs.

Deposited carbon on the catalyst surface can generally be classified into amorphous carbon and graphitic carbon. Amorphous carbon is formed through the adsorption of carbon species on active nickel sites; it is highly reactive and can be removed at relatively low temperatures [8]. In heterogeneous catalysis, carbon deposits of different structural order can form on catalyst surfaces, and their nature strongly affects catalyst stability and activity. Amorphous carbon species are generally less ordered and more reactive, whereas graphitic carbon exhibits a more ordered sp^2-bonded lattice that is thermodynamically stable and harder to remove by simple low-temperature treatments [9]. Such graphitic deposits tend to form at higher reaction temperatures and, once present, require significantly higher temperatures or aggressive regeneration procedures for elimination. As carbon continues to accumulate, these graphitic coke species block active sites or pores and physically limit the access of reactant gases to catalytic centers, which leads to a gradual decline in catalytic activity and, in severe cases, complete catalyst deactivation [10].

As a result, the growth rate of CNTs decreases, their length shortens, graphitization becomes limited, and both electrical and thermal properties deteriorate [11]. Therefore, the controlled removal or prevention of amorphous carbon formation during synthesis is one of the most effective strategies for improving CNT quality.

Several approaches have been explored for the elimination of amorphous carbon. One of the most widely studied techniques involves oxidative acid treatments, using mixtures of nitric acid (HNO_3), sulfuric acid (H_2SO_4), or hydrogen peroxide (H_2O_2) [12–14]. By functionalization, chemical groups such as carboxyl (–COOH), carbonyl (–CO), and hydroxyl (-OH) are formed on the CNT surfaces, which exfoliate the CNT bundles, improve their wettability and enable their dispersion in polar media. In the presence of metal precursors, these surface groups help the diffusion and nucleation of metals on the CNT sidewalls for the synthesis of ideal CNT composites [15]. The acidic treatment tends to damage the external graphitic lattice structure of CNTs[16]. Thus, optimizing the concentration and duration of oxidation is crucial [17].

Cite as: S.G. Gulomjanova, I.Kh. Khudaykulov, I.J. Abdisaidov, Kh.B. Ashurov, East Eur. J. Phys. 1, 357 (2026), https://doi.org/10.26565/2312-4334-2026-1-42

An alternative approach is the Water-Assisted Chemical Vapor Deposition (WA-CVD) method, where water vapor (H_2O) is introduced into the synthesis environment. Adding water vapor to the CVD process can improve the CNT purity, alignment, and growth height by removing amorphous carbon on the (typically Fe) catalyst particles owing to the partial oxidation of the metallic catalyst. [18,19]. This method enables the formation of vertically aligned, dense, and highly ordered CNT arrays [20]. Studies have shown that samples synthesized at higher temperatures (600–800°C) exhibit a higher degree of graphitization, whereas lower temperatures favor amorphous carbon formation [21].

Moreover, the choice of metal catalyst significantly influences amorphous carbon formation. Transition metals such as Fe, Co, and Ni effectively decompose carbon and promote diffusion; however, at lower growth temperatures, amorphous carbon deposition becomes more likely [22]. Therefore, the activation and cleanliness of the catalyst surface play a crucial role in CNT growth [23].

Recent research demonstrates that the *in-situ* removal of amorphous carbon—during rather than after synthesis—enhances the morphology, graphitization, and functional performance of CNTs [24,25]. This not only simplifies the synthesis process but also minimizes subsequent chemical treatments, preserving the structural integrity of the nanotubes.

In this study, the conventional CVD and water-assisted CVD (WA-CVD) methods are compared to evaluate the influence of water vapor on amorphous carbon formation at low temperatures. The presence of water vapor facilitates the decomposition of excess amorphous carbon on the catalyst surface in real time, keeping active sites exposed. Consequently, CNT growth yield increases, catalyst lifetime extends, and graphitization improves. Understanding the mechanism of amorphous carbon formation and its suppression via WA-CVD or oxidative environments provides a pathway for producing low-defect, highly crystalline CNTs at relatively low temperatures.

This approach establishes an important scientific foundation for the development of efficient, stable, and thermally conductive nanotubes for thermal interface materials (TIMs) [26], nanocomposites [27], and electronic devices [28].

In this study, reduced nickel nanocatalysts synthesized via the sol–gel method were employed for the growth of carbon nanotubes (CNTs). Nickel(II) nitrate hexahydrate [$Ni(NO_3)_2 \cdot 6H_2O$] was dissolved in distilled water, and ammonium hydroxide (NH_4OH) was gradually added until the pH reached 11. The resulting solution was slowly heated to 85 °C, leading to the formation of a gel. The obtained gel was deposited onto sapphire substrates using the spin-coating technique and subsequently dried at 400 °C. The nickel nanocatalysts were produced by reducing nickel oxide (NiO) at elevated temperatures in a hydrogen atmosphere, which converted NiO into metallic nickel and enhanced its catalytic activity.

EXPERIMENT

Carbon nanotubes were synthesized on Ni-coated sapphire substrates using a super-growth chemical vapor deposition (CVD) technique that selectively removes amorphous carbon without damaging the nanotube structure at the growth temperature. The schematic diagram of the experimental setup developed for CNT synthesis using the super-growth CVD method is shown in Figure 1.

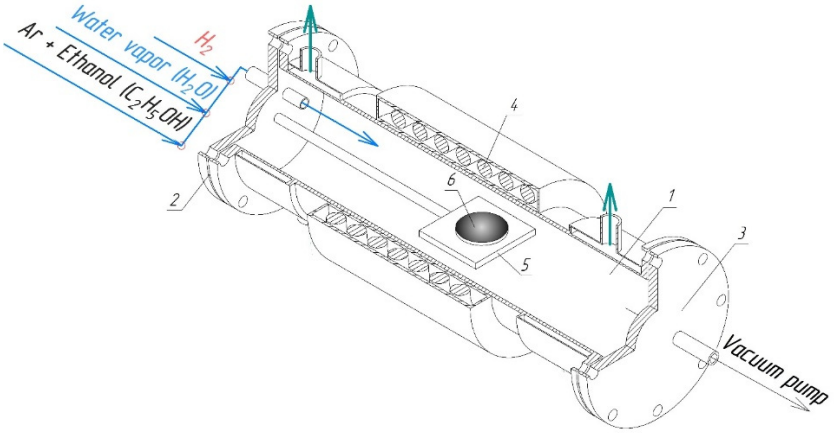

Figure 1. Schematic diagram of the designed CVD system: 1– quartz reactor (1 m length); 2, 3 – flanges; 4 – laboratory furnace; 5 – molybdenum plate with thermocouple; 6 – sample

All experiments were conducted under identical reaction conditions, with the only difference being the presence or absence of water vapor during the growth stage. The substrates were placed inside a quartz-tube furnace, and when the reaction temperature reached 550 °C, ethanol (C_2H_5OH) was introduced into the reactor together with argon gas, maintaining a total gas flow rate of 3.0 L/min. The reaction time was fixed at 45 minutes. CNT growth was performed under two different conditions:

-Dry growth (without water vapor): Ar (2900 sccm) + C_2H_5OH (100 sccm).

-Water-assisted growth (WA-CVD): H_2O + Ar (2900 sccm) + C_2H_5OH (100 sccm).

In the WA-CVD process, deionized water at room temperature was passed through a bubbler to generate water vapor, which was continuously monitored and controlled. The controlled addition of water vapor served to maintain the catalyst activity and enhance the growth rate of carbon nanotubes.

After 45 minutes of growth, the flow of C_2H_5OH and Ar was stopped, and the samples were allowed to cool naturally to room temperature.

To evaluate the structural, crystallographic, and morphological properties of the synthesized carbon nanotubes (CNTs), several advanced characterization techniques were employed.

Raman spectroscopy was carried out using a *Renishaw Raman spectrometer* equipped with a 532 nm laser source operating at 100% power (approximately 10 mW). The spectra were recorded over the range of 100–3500 cm^{-1}. This analysis provided insights into the degree of graphitization, the presence of amorphous carbon, and defects within the CNT structure.

The crystalline structure and phase composition of the CNTs were analyzed using *Rigaku SmartLab SE X-ray Diffractometer with Guidance Software*. Measurements were conducted with Cu Kα radiation (λ = 1.5406 Å) at an operating voltage of 40 kV and current of 50 mA. Scans were performed in 1D mode, with a step size of 0.01° and a scan rate of 3.00° min^{-1}, covering the 2θ range of 10°–100°.

To further investigate the morphology and internal structure, Transmission Electron Microscopy (TEM) analysis was performed using a *Thermo Scientific Talos F200i (S)* field-emission scanning TEM operating at 20–200 kV.

RESULTS AND DISCUSSION

The Raman spectra of the synthesized carbon nanotubes (CNTs) exhibited three characteristic peaks typical of carbon nanomaterials — the D, G, and 2D bands — as shown in Figure 2. These peaks correspond to the vibrational modes of *sp^2-hybridized carbon atoms* within the graphitic lattice, confirming that the nanotubes possess a graphitic structure.

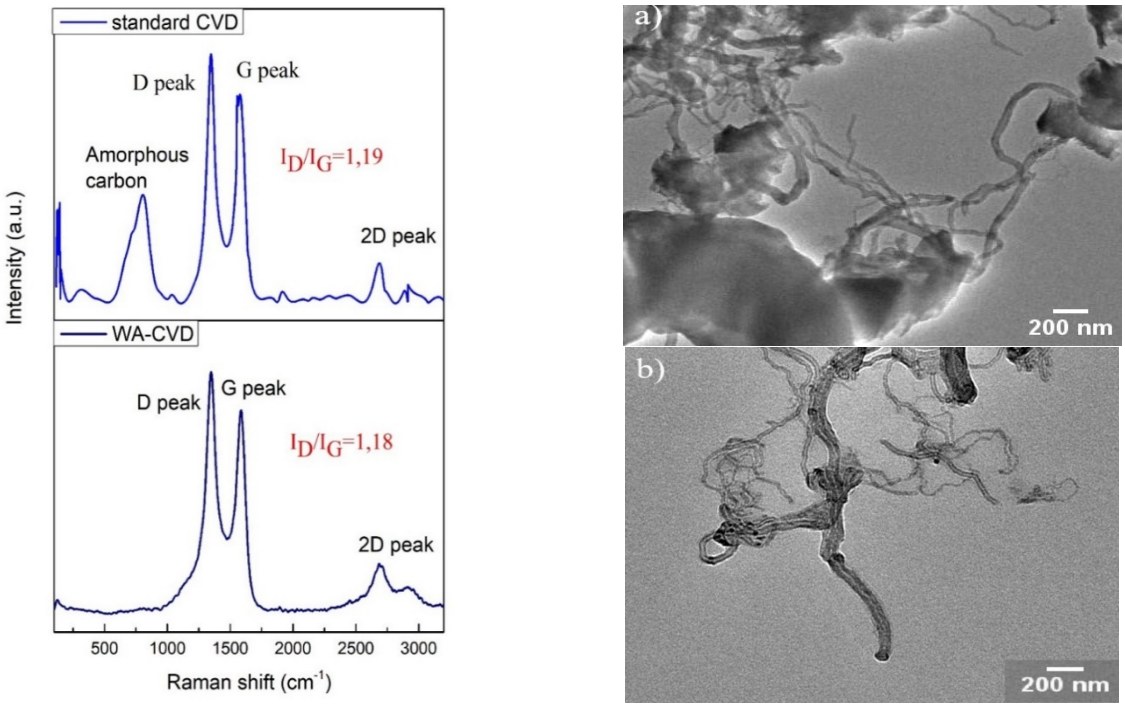

Figure 2. Raman spectra and TEM image of carbon nanotubes synthesized by: (a) conventional CVD and (b) water-assisted CVD (WA-CVD) methods

In the Raman spectra, the G band observed in the range of 1575–1586 cm^{-1} corresponds to the in-plane stretching vibrations of sp^2-bonded carbon atoms, confirming the presence of a crystalline graphitic structure. The D band (~1343-1349 cm^{-1}) is associated with lattice imperfections and amorphous phases, and its intensity reflects the degree of structural disorder in the sample.

For the CNTs grown by the conventional CVD method, the D, G, and 2D peaks were observed at 1343, 1575, and 2685 cm^{-1}, respectively, with an I_D/I_G ratio of approximately 1.19, indicating the presence of defects and amorphous carbon. Additionally, a low-frequency radial breathing mode (RBM) in the range of 126–139 cm^{-1} confirmed the existence of single-walled carbon nanotube (SWCNT) fractions.

In contrast, for the CNTs synthesized using the WA-CVD method, the D, G, and 2D peaks appeared at 1349, 1586, and 2686 cm^{-1}, respectively, while the characteristic amorphous carbon signal around ~794 cm^{-1} was absent, indicating higher purity of the sample. The $I_D/I_G \approx 1.18$ value suggests improved crystallinity. The rightward shift of the G-band to 1586 cm^{-1} can be attributed to mechanical compression or doping-induced stress within the carbon lattice.

The X-ray diffraction (XRD) patterns of the CNTs synthesized under both conditions are shown in Figure 3. The diffractograms exhibited several distinct peaks in the 2θ range of 10°–100°, confirming the crystalline nature of the obtained samples.

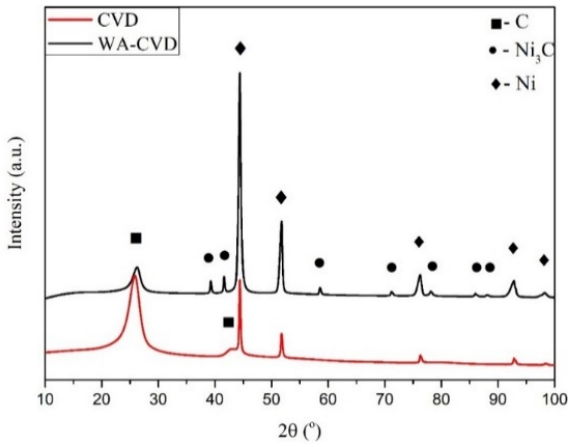

Figure 3. XRD diffractograms of carbon nanotubes synthesized by conventional CVD (red) and WA-CVD (black) methods

In the diffractogram of the CNTs synthesized by the conventional CVD process, the main diffraction peaks appeared at 2θ ≈ 25.8°, 42.8°, 44.4°, 51.7°, 76.2°, 92.8°, and 98.3°, corresponding respectively to the (002) and (020) planes of graphitic carbon and to the (111), (200), (220), (311), and higher-order reflections of metallic Ni phases (JCPDS №. 04-0850). The strong peak near 2θ ≈ 25.8° confirms the presence of graphitic carbon layers, indicating the formation of carbon nanostructures.

The XRD pattern of CNTs synthesized via the WA-CVD method exhibited the same major peaks (2θ = 26.27°, 44.4°, 76.2°, 92.8°, and 98.3°) along with several additional reflections at 2θ ≈ 39.3°, 41.6°, 58.62°, 71.20°, 78.11°, 86.05°, 88.09°, and 97.49°. These additional peaks correspond to the hexagonal Ni_3C phase (PDF No. 77-0194), indexed to the(110), (006), (116), (300), and (119) planes [29].

The (002) peak of CNTs grown under standard CVD conditions appeared at 2θ ≈ 26°, typical for graphitic carbon structures. In contrast, for CNTs synthesized under WA-CVD conditions, a slight rightward shift of the (002) peak to 2θ ≈ 26.2° was observed, which is attributed to lattice parameter contraction. The primary causes of this shift are the compressive stresses induced on the catalyst surface by the water vapor, a reduction in nanocrystallite size, and possible atomic rearrangements caused by oxidation or doping processes, leading to a decrease in interatomic spacing and, consequently, an increase in the Bragg angle (2θ) [30].

The morphological characteristics of the synthesized CNTs were further investigated using Transmission Electron Microscopy (TEM), as shown in Figure 2 and Figure 4.

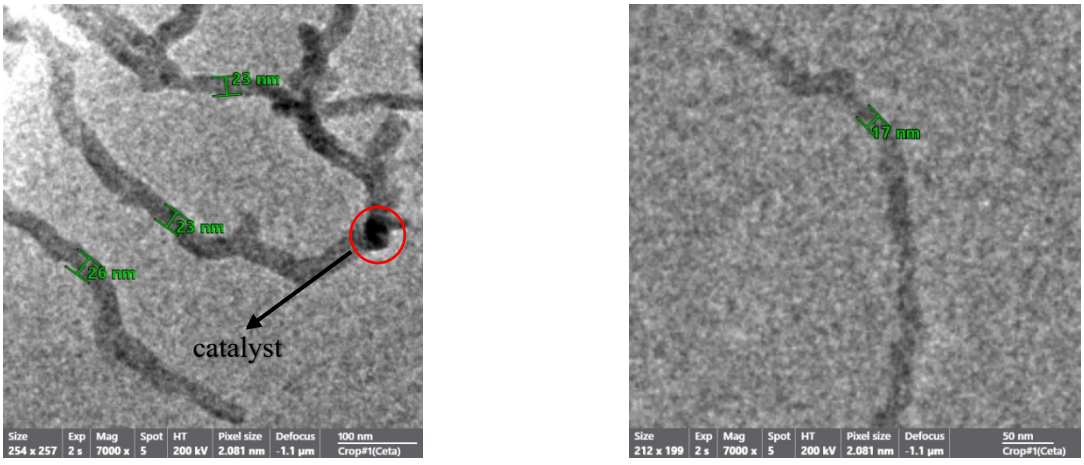

a) b)

Figure 4. TEM images of carbon nanotubes: (a) CNTs synthesized by the conventional CVD method; (b) CNTs synthesized by the water-assisted CVD (WA-CVD) method

The TEM image of the sample grown under dry CVD conditions (Fig. 2a) shows nanotubes covered with a thick layer of amorphous carbon and agglomerated clusters. The nanotubes have diameters of approximately 23–40 nm (Fig. 4a) and lengths typically limited to 200–500 nm. The presence of numerous irregular and fragmented segments indicates uncontrolled carbon deposition on the catalyst surface, leading to the accumulation of amorphous carbon and consequently to CNTs of poor structural quality with disordered morphology.

In contrast, the TEM image of the sample synthesized under WA-CVD conditions (Figure 2b) shows much cleaner and more ordered nanotubes. The CNTs are thinner and longer, with diameters ranging from 17–25 nm (Fig. 4b) and lengths exceeding several micrometers (≥1 µm). The amorphous carbon layer is almost absent, and the CNTs are well-

separated from one another. This demonstrates that water vapor regenerates the catalyst surface, suppresses excessive carbon deposition, and stabilizes the growth process.

From the TEM images (Figures 4a and 4b), it can be concluded that CNTs synthesized by both the CVD and WA-CVD methods grew via the tip-growth mechanism. In both cases, Ni nanoparticles served as active catalytic centers, decomposing the carbon precursor and promoting tubular carbon formation.

Overall, the comparative analysis indicates that synthesis performed in the presence of water vapor results in higher-quality, longer, and purer carbon nanotubes than those obtained under dry conditions. Water vapor not only extends the catalyst lifetime but also produces CNTs with smaller diameters and more uniform distributions.

CONCLUSIONS

The conducted research demonstrated that the water-assisted chemical vapor deposition (WA-CVD) method is significantly more efficient than the conventional CVD process for synthesizing carbon nanotubes (CNTs). The Raman analysis showed that CNTs synthesized under WA-CVD conditions exhibited no amorphous carbon components and displayed a higher degree of graphitic ordering ($I_D/I_G \approx 1.18$). The XRD results revealed a shift of the (002) peak to $2\theta = 26.2°$ and the formation of the Ni_3C phase, confirming the stabilizing effect of water vapor on catalyst activity. The TEM observations demonstrated that CNTs grown by the WA-CVD method were thin (5–12 nm), long (≥1 μm), and well-separated, whereas those grown under conventional CVD conditions were short, irregular, and coated with amorphous carbon. Overall, water vapor regenerates the catalyst surface, suppresses amorphous carbon formation, and improves both graphitization and growth efficiency. Therefore, the WA-CVD method has been proven to be an optimal approach for synthesizing thin, long, and well-aligned carbon nanotubes with high crystallinity and purity.

Acknowledgments

The authors gratefully acknowledge the financial and technical support provided by the Ministry of Higher Education, Science, and Innovation under project number IL-5421101842.

ORCID

Sevara G. Gulomjanova, https://orcid.org/0009-0001-1760-9766; **Ilyos Kh. Khudaykulov,** https://orcid.org/0000-0002-2335-4456; **Ilyos J. Abdisaidov,** https://orcid.org/0000-0001-7473-1074; **Khatam B. Ashurov,** https://orcid.org/0000-0002-7604-2333

REFERENCES

[1]. S. Iijima, "Helical microtubules of graphitic carbon," Nature, **354**, 56–58 (1991). https://doi.org/10.1038/354056a0
[2]. M.S. Dresselhaus, G. Dresselhaus, and P. Avouris, *Carbon Nanotubes: Synthesis, Structure, Properties, and Applications*, (Springer, Berlin, 2001). https://doi.org/10.1007/3-540-39947-X
[3]. R.H. Baughman, A.A. Zakhidov, and W.A. de Heer, "Carbon nanotubes – the route toward applications," Science, **297**, 787–792 (2002). https://doi.org/10.1126/science.1060928
[4]. J. Robertson, "Growth of carbon nanotubes for electronics," Materials Today, **10**, 36–43 (2007). https://doi.org/10.1016/S1369-7021(06)71790-4
[5]. A. Peigney, C. Laurent, E. Flahaut, R.R. Bacsa, and A. Rousset, "Specific surface area of carbon nanotubes and bundles of carbon nanotubes," Carbon, **39**, 507–514 (2001). https://doi.org/10.1016/S0008-6223(00)00155-X
[6]. D. Tasis, N. Tagmatarchis, A. Bianco, and M. Prato, "Chemistry of carbon nanotubes," Chemical Reviews, **106**, 1105–1136 (2006). https://doi.org/10.1021/cr050569o
[7]. R. Andrews, D. Jacques, D. Qian, and T. Rantell, "Multiwall carbon nanotubes: synthesis and application," Carbon, **39**, 1681-1687 (2001). https://doi.org/10.1021/ar010151m
[8]. I.J. Abdisaidov, S.G. Gulomjanova, I.Kh. Khudaykulov, and K.B. Ashurov, "Low-temperature growth of carbon nanotubes using nickel catalyst," East European Journal of Physics, (3), 355–358 (2024). https://doi.org/10.26565/2312-4334-2024-3-41
[9]. H. Qu, *et al*. "Reconfiguring organic color centers on the sp^2 carbon lattice of single-walled carbon nanotubes," ACS nano, **16**(2), 2077-2087 (2022). https://doi.org/10.1021/acsnano.1c07669
[10]. E.T.C. Vogt, D. Fu, B.M. Weckhuysen, "Carbon deposit analysis in catalyst deactivation, regeneration, and rejuvenation," Angewandte Chemie International Edition, 62(29), e202300319 (2023). https://doi.org/10.1002/anie.202300319
[11]. S. Maruyama, R. Kojima, Y. Miyauchi, S. Chiashi, and M. Kohno, "Low-temperature synthesis of high-purity single-walled carbon nanotubes from alcohol," Chemical Physics Letters, **360**, 229–234 (2002). https://doi.org/10.1016/S0009-2614(02)00838-2
[12]. A. Reina, M. Hofmann, D. Zhu, and J. Kong, "Growth mechanism of long and horizontally aligned carbon nanotubes by chemical vapor deposition," Journal of Physical Chemistry C, **111**(20), 7292–7297 (2007). https://doi.org/10.1021/jp0711500
[13]. K. Hata, D.N. Futaba, K. Mizuno, T. Namai, M. Yumura, and S. Iijima, "Water-assisted highly efficient synthesis of impurity-free single-walled carbon nanotubes," Science, **306**, 1362–1364 (2004). https://doi.org/10.1126/science.1104962
[14]. T. A. Saleh, "The influence of treatment temperature on the acidity of MWCNT oxidized by HNO_3 or a mixture of HNO_3/H_2SO_4," Applied Surface Science, **257**(17), 7746–7751 (2011). https://doi.org/10.1016/j.apsusc.2011.04.020
[15]. N. Sezer, and M. Koç, "Oxidative acid treatment of carbon nanotubes," Surfaces and Interfaces, 14, 1–8 (2019). https://doi.org/10.1016/j.surfin.2018.11.001
[16]. L. Lavagna, M. Bartoli, D. Suarez-Riera, D. Cagliero, S. Musso, and M. Pavese, "Oxidation of Carbon Nanotubes for Improving the Mechanical and Electrical Properties of Oil-Well Cement-Based Composites," ACS Applied Nano Materials, **5**(5), 6671-6678 (2022). https://doi.org/10.1021/acsanm.2c00706
[17]. G. Gao, M. Pan, and C. D. Vecitis, "Effect of the oxidation approach on carbon nanotube surface functional groups and electrooxidative filtration performance," Journal of Materials Chemistry A, **3**(14), 7575–7582 (2015). https://doi.org/10.1039/C4TA07191C

[18]. K. Strobl, and F. Rajab, "Water-Assisted Catalytic VACNT Growth Optimization for Speed and Height," Processes, **11**(6), 1587 (2023). https://doi.org/10.3390/pr11061587
[19]. D. N. Futaba, K. Hata, T. Yamada, K. Mizuno, M. Yumura, and S. Iijima, "Kinetics of water-assisted single-walled carbon nanotube synthesis revealed by a time-evolution analysis," Physical Review Letters, **95**(5), 056104 (2005). https://doi.org/10.1103/PhysRevLett.95.056104
[20]. Y. Yun, V. Shanov, Y. Tu, S. Subramaniam, and M.J. Schulz, "Growth mechanism of long aligned multiwall carbon nanotube arrays by water-assisted chemical vapor deposition," The Journal of Physical Chemistry B, **110**(47), 23920–23925 (2006). https://doi.org/10.1021/jp057171g
[21]. L. Dong, J. G. Park, B. E. Leonhardt, S. Zhang, and R. Liang, "Continuous synthesis of double-walled carbon nanotubes with water-assisted floating catalyst chemical vapor deposition," Nanomaterials, **10**(2), 365 (2020). https://doi.org/10.3390/nano10020365
[22]. A. Ismatov, C. Romanitan, K. Ashurov, M. Adilov, and A. Rahimov, "Annealing-induced morphological evolution of iron nanocatalysts for carbon nanotube growth," Eurasian Physical Technical Journal, **22**(3 (53)), 5–13 (2025). https://doi.org/10.31489/2025N3/5-13
[23]. P. Nikolaev, M.J. Bronikowski, R.K. Bradley, F. Rohmund, D.T. Colbert, K.A. Smith, and R.E. Smalley, "Gas-phase catalytic growth of single-walled carbon nanotubes from carbon monoxide," Chemical Physics Letters, **313**, 91–97 (1999). https://doi.org/10.1016/S0009-2614(99)01029-5
[24]. Z. Chen, X. Wei, S. Lu, J. Ding, N. Du, C. Feng, K. Chen, *et al*., "Surface in-situ graphitization and properties of amorphous carbon film induced by laser irradiation," Friction, **13**(6), (2025). https://doi.org/10.26599/FRICT.2025.9440977(12)
[25]. R. Xu, H. Yin, D. He, X. Ma, S. Liang, C. Jin, and X. Chen, "Mechanism of polymer removal from semiconducting single-walled carbon nanotubes via rapid thermal processing: insights from in situ environmental transmission electron microscopy," Nanoscale, **17**, 14941–14947 (2025). https://doi.org/10.1039/D5NR01566A
[26]. D. Fabris, M. Rosshirt, C. Cardenas, P. Wilhite, T. Yamada, and C.Y. Yang, "Application of carbon nanotubes to thermal interface materials," Journal of Electronic Packaging, 020902(6), (2011). https://doi.org/10.1115/1.4003864
[27]. Z. Zhang, N. Zhang, and Z. Zhang, "High-Performance Carbon Nanotube Electronic Devices: Progress and Challenges," Micromachines, **16**(5), 554 (2025). https://doi.org/10.3390/mi16050554
[28]. E. W. Fenta, and B. A. Mebratie, "Advancements in carbon nanotube-polymer composites: Enhancing properties and applications through advanced manufacturing techniques," Heliyon, **10**, (e36490) (2024). https://doi.org/10.1016/j.heliyon.2024.e36490
[29]. Y. Zhang, Y. Zhu, Y. Cao, D. Li, Z. Zhang, K. Wang, F. Ding, *et al*., "Size and morphology-controlled synthesis of Ni_3C nanoparticles in a TEG solution and their magnetic properties," RSC Advances, **6**, (2016). https://doi.org/10.1039/C6RA11916F
[30]. A. Cao, C. Xu, J. Liang, D. Wu, and B. Wei, "X-Ray Diffraction Characterization on the Alignment Degree of Carbon Nanotubes," Chemical Physics Letters, **344**(1-2), 13–17 (2001). https://doi.org/10.1016/S0009-2614(01)00671-6

ПОКРАЩЕННЯ СИНТЕЗУ ВУГЛЕЦЕВИХ НАНОТРУБОК ШЛЯХОМ ВИДАЛЕННЯ АМОРФНОГО ВУГЛЕЦЮ

Севара Г. Гуломджанова, Ільос Х. Худайкулов, Ільос Дж. Абдісаїдов, Хатам Б. Ашуров
Інститут іонно-плазмових та лазерних технологій ім. Аріфова Академії наук Узбекистану
100125, вул. Дурмон йулі, 33, Ташкент, Узбекистан

У цьому дослідженні вуглецеві нанотрубки (ВНТ) були синтезовані на сапфірових підкладках з нікелевим покриттям за допомогою традиційних методів та методів хімічного осадження з парової фази з використанням води (CVD та WA-CVD) для оцінки впливу водяної пари на видалення аморфного вуглецю та активність каталізатора за низьких температур. Відновлені нікелеві нанокаталізатори були отримані золь-гель методом та активовані в атмосфері водню. Раманівська спектроскопія підтвердила, що вуглецеві нанотрубки, синтезовані методом WA-CVD, демонструють вищий ступінь графітизації (ID/IG ≈ 1,18) та відсутність піків аморфного вуглецю близько 794 $см^{-1}$, що свідчить про покращену чистоту. Рентгенівський дифракційний аналіз (XRD) виявив утворення графітових вуглецевих (002) та кристалічних фаз Ni_3C, а також зсув піку (002) праворуч до $2\theta = 26{,}2°$, що свідчить про стиснення кристалічної решітки, спричинене напруженням, індукованим водяною парою. Зображення просвічувальної електронної мікроскопії (TEM) показали, що вуглецеві нанотрубки, синтезовані в умовах WA-CVD, були тоншими (17–25 нм), довшими (≥ 1 мкм) та чистішими, ніж ті, що були отримані звичайним CVD, які демонстрували товсті покриття з аморфного вуглецю. Ці результати демонструють, що контрольоване додавання водяної пари під час CVD пригнічує утворення аморфного вуглецю, регенерує активні центри каталізатора та значно покращує кристалічність та морфологічну однорідність вуглецевих нанотрубок. Отримані результати пропонують ефективний підхід до синтезу високочистих, добре вирівняних вуглецевих нанотрубок, придатних для використання в термоінтерфейсних матеріалах, нанокомпозитах та електронних пристроях.

Ключові слова: *вуглецеві нанотрубки; видалення аморфного вуглецю; CVD з використанням води; нікелевий каталізатор; золь-гель синтез; раманівська спектроскопія; рентгенівська дифракція; морфологія TEM; ступінь графітизації; регенерація каталізатора*